

N. KALIVAS¹
I. VALAIS^{2,4}
D. NIKOLOPOULOS²
A. KONSTANTINIDIS²
A. GAITANIS^{2,5}
D. CAVOURAS²
C.D. NOMICOS³
G. PANAYIOTAKIS⁴
I. KANDARAKIS^{2,✉}

Light emission efficiency and imaging properties of YAP:Ce granular phosphor screens

¹ Greek Atomic Energy Commission, P.O. Box 60092, 15310 Agia Paraskevi, Greece
² Department of Medical Instrumentation Technology, Technological Educational Institution of Athens, Agiou Spyridonos, 12210 Athens, Greece
³ Department of Electronics, Technological Educational Institution of Athens, Athens, Greece
⁴ Department of Medical Physics, School of Medicine, University of Patras, 26500 Patras, Greece
⁵ Foundation for Biomedical Research of the Academy of Athens (IIBEAA), Soranou Efessiou 4, Athens 11527, Greece

Received: 12 December 2006 / Accepted: 4 June 2007
Published online: 14 July 2007 • © Springer-Verlag 2007

ABSTRACT Phosphor materials are used in medical imaging combined with radiographic film or other photodetectors. Cerium (Ce^{3+})-doped scintillators are of particular interest for medical imaging, because of their very fast response. YAP:Ce scintillator-based image detectors have already been evaluated in single-crystal form and under conditions of positron emission tomography and synchrotron or γ -ray irradiation. Furthermore, YAP:Ce phosphor has been evaluated in conjunction with radiographic films. The present work reports experimental and theoretical data concerning the light output absolute luminescence efficiency (AE) of the YAP:Ce screens under irradiation conditions employed in medical X-ray projection imaging (i.e., in diagnostic radiology), projection imaging (i.e., in diagnostic radiology). YAP:Ce phosphor screens with surface densities ranging between 53 and 110 mg/cm^2 were prepared by sedimentation on fused silica substrates in our laboratory. The resulted surface density of the screens was determined by dividing the phosphor mass deposited on the screen surface with the area of the surface. Additionally this work addresses the imaging performance of YAP:Ce by estimation of the detective quantum efficiency (DQE), i.e., the square of the signal to noise ratio transfer. Absolute efficiency was found to decrease with X-ray tube voltage for YAP:Ce phosphor. The highest experimental efficiency was obtained for the 53.7 mg/cm^2 and 88.0 mg/cm^2 YAP:Ce screens. The highest DQE value was found for the 88.0 mg/cm^2 screen irradiated at 60 kVp.

PACS 81.05.Zx; 87.59.-e; 87.57.Ce

(300–450 nm) with a decay time of 30 ns [4, 5]. These properties are attractive for X-ray imaging since: (i) their light spectrum is compatible to several existing optical sensors (i.e., photocathodes, radiographic films) and ii) fast decay time is a prerequisite for dynamic real-time imaging. YAP:Ce scintillator based image detectors have already been reported in the literature [4, 5]. These detectors, however, employed YAP:Ce in single-crystal form and have been evaluated under conditions of positron emission tomography and synchrotron or γ -ray irradiation [4–7]. The imaging capability of YAP:Ce detectors has been tested in terms of parameter determination such as light yield (light photons/MeV) and spatial resolution [4–7]. A previous study of our group reported an experimental evaluation of YAP:Ce phosphor screens under diagnostic radiology conditions [8]. In the aforementioned study, various YAP:Ce screen layers were combined to blue sensitivity radiographic films and evaluated in terms of radiographic response, modulation transfer function (MTF) and noise transfer function (NTF) [8]. To our knowledge YAP:Ce powder scintillator (phosphor) is yet to be fully studied for use either in digital or in conventional diagnostic radiology detectors. The present work reports experimental and theoretical data concerning the light output absolute luminescence efficiency (AE) of the YAP:Ce screens under irradiation conditions employed in medical X-ray projection imaging (i.e., in diagnostic radiology). Additionally this work addresses the imaging performance of YAP:Ce by estimation of the detective quantum efficiency (DQE), i.e., the square of the signal to noise ratio transfer. DQE was further estimated in the spatial frequency domain.

1 Introduction

Scintillators, or phosphors, coupled to optical sensors (photodiodes, photocathodes, films etc) are employed in most radiation detectors used in medical imaging systems [1]. Cerium (Ce^{3+})-doped scintillators are of particular interest for medical imaging, because of their very fast response. The latter is due to an electric dipole transition in Ce ion [2, 3]. $\text{YAlO}_3:\text{Ce}$ (YAP:Ce) (cerium-doped yttrium aluminum oxide) is a scintillator emitting blue light

2 Materials and methods

This work evaluates the performance of YAP:Ce phosphor screens for use in medical imaging X-ray detectors. To this purpose some physical parameters related to the light emission efficiency and to the imaging performance of this phosphor were examined. First, the absolute luminescence efficiency was studied. This efficiency is defined as $\text{AE} = \Psi_L/X$, where Ψ_L is the light energy flux emitted by an excited phosphor and X is the incident exposure rate. AE characterizes the ability of a phosphor screen-based X-ray image

✉ Fax: +30210 5385387, E-mail: kandarakis@teiath.gr

detector to produce an adequately bright image at reduced patient dose. Furthermore the detective quantum efficiency, describing the signal-to-noise ratio transfer from the input to the output, was estimated. This was achieved by using data obtained from the experimental and theoretical determination of AE. DQE is defined as [1, 9] $DQE = [SNR_0/SNR_1]^2$, where SNR_0 , SNR_1 are the output and input signal to noise ratios, respectively. DQE is an overall image quality metric, which may be expressed in the Fourier spatial frequency domain as a function of the signal and the noise transfer functions, and describes the signal-to-noise-ratio transfer from the input to the output [1, 9].

2.1 Theoretical model

2.1.1 Absolute luminescence efficiency (AE). The absolute luminescence efficiency, of a phosphor screen of thickness T , irradiated by X-ray photons of energy E was theoretically evaluated [9] in terms of intrinsic physical properties, using the following relation

$$AE = n_Q(E, T)n_C G_1(\sigma, \beta, \varrho, T), \quad (1)$$

where $n_Q(E, T)$ is the fraction of the incident X-ray energy which is deposited in the phosphor material, n_C , is the intrinsic X-ray to light conversion efficiency giving the fraction of deposited X-ray energy transformed into light photon energy and $G_1(\sigma, \beta, \varrho, T)$ is the light transmission efficiency, expressing the fraction of the light produced that reaches the screen output. σ , β and ϱ are optical parameters related to light absorption, light scattering and light reflectivity in the phosphor material [9–11]. Assuming one-dimensional radiation transfer, one can describe AE with a one-dimensional model for X-ray and light propagation in a phosphor screen as [9, 11]

$$AE = \frac{n_C \gamma t_r \mu(E)(1 + \varrho)e^{-\mu(E)T}}{2(\mu(E)^2 - \sigma^2)} \times \frac{\left[(\mu(E) - \sigma)(1 - \beta)e^{-\sigma T} + 2(\sigma + \mu(E)\beta)e^{\mu(E)T} - (\mu(E) + \sigma)(1 + \beta)e^{\sigma T} \right]}{(1 + \beta)(\varrho + \beta)e^{\sigma T} - (1 - \beta)(\varrho - \beta)e^{-\sigma T}}, \quad (2)$$

where $\mu(E)$ is the X-ray energy absorption coefficient, which expresses the probability per unit of surface density that the X-rays will deposit their energy in the medium [12], γ is a conversion factor converting energy fluence (W/m^2) into exposure rate (mR/s) t_r is the transparency of the phosphor screen substrate. If the energy spectrum of X-rays, $f(E)$, is to be taken into account, then AE can be calculated by summing over this spectrum, up to the peak energy (kVp) of the X-ray spectrum:

$$AE_{kVp} = \frac{\sum_E f(E)AE}{\sum_E f(E)}, \quad (3)$$

where kVp denotes the high voltage (kilovolt peak) applied to the X-ray tube. This voltage is equal to the maximum energy of the X-ray spectrum.

2.1.2 Detective quantum efficiency evaluation. It has been shown in the literature that frequency depended DQE(u) can be written as [13, 14]

$$DQE(u) = F \left(\frac{d\Phi_1}{dF} \right)^2 \frac{MTF(u)^2}{NPS(0)NTF(u)^2}, \quad (4)$$

where u is the spatial frequency, F is the X-ray photon fluence incident on the screen surface, i.e., $\sum_E f(E)$ in (3), and Φ_1 is the optical photon fluence. MTF denotes the modulation transfer function, which describes the efficiency of signal transfer as a function of spatial frequency. MTF indicates spatial resolution deterioration from the input to the output of an imaging system. NPS denotes the noise power spectrum, which expresses the noise variations in terms of spatial frequency and indicates image detectability and NTF is the corresponding noise transfer function.

Calculation of MTF, NPS and Φ_1 . Lets assume an X-ray fluence distribution, $f(E)$, incident on the surface of a phosphor screen of thickness T . A fraction, $q(t, E)$, of the absorbed X-ray photons, (e.g., a fraction of the product $f(E)n_Q(E, T)$), will deposit an amount of energy in a thin layer dt at depth t . This energy will then produce optical photons. The fraction $q(t, E)$ may be calculated by the following expression [11, 13, 14]

$$q(t, E) = \frac{f(E)e^{-\mu(E)t}\mu(E)dt}{f(E)n_Q(E, T)}. \quad (5)$$

The number of optical photons produced inside a phosphor screen depends upon the intrinsic quantum gain, $m_0(E)$, of the phosphor. The latter is equal to the fraction of absorbed X-ray photon energy converted into light within the scintillator's mass, divided by the mean energy of the emitted optical photons E_λ [13, 14]:

$$m_0(E) = n_C \frac{E}{E_\lambda}. \quad (6)$$

The number of emitted optical photons, created at depth t and transmitted through the rest of the screen thickness ($T-t$), may be expressed in the spatial frequency domain by a function $M(u, E, t)$, given by the following product [9, 13, 14]

$$M(u, E, t) = f(E)n_Q(E, T)q(t, E)m_0(E)G_1(\sigma, \beta, \varrho, u, t), \quad (7)$$

where $G_1(\sigma, \beta, \varrho, u, t)$ expresses the Fourier transform of the light burst distribution of the optical quanta originating from depth between t and $t + dt$ end escaping to the output per X-ray absorbed.

$G_1(\sigma, \beta, \varrho, u, t)$ can be written [9, 13, 14] as the product of the number of the optical photons originating from a depth between t and $t + dt$ end escaping to the output, denoted as $G_1(\sigma, \beta, \varrho, t)$, multiplied by the modulation transfer function of a thin layer positioned at depth between t and $t + dt$. That is $G_1(\sigma, \beta, \varrho, u, t) = G_1(\sigma, \beta, \varrho, t)MTF(u, t)$. Since at zero spatial frequency $MTF = 1$, $G_1(\sigma, \beta, \varrho, t)$ can be estimated as $G_1(\sigma, \beta, \varrho, u = 0, t)$ [13, 14]. $G_1(\sigma, \beta, \varrho, u, t)$ can be calculated as [8, 11, 13]

$$G_1(\sigma, \beta, \varrho, u, t) = \frac{\sigma\varrho[(b\beta + \sigma)e^{bt} + (b\beta - \sigma)e^{-bt}]}{(b\beta + \sigma)(b\beta + \sigma\varrho)e^{bT} - (b\beta - \sigma)(b\beta - \sigma\varrho)e^{-bT}}, \quad (8)$$

where $b^2 = \sigma^2 + 4\pi^2(u/d)^2$, d is the density of the phosphor material. Equation (8) is valid under the following assumptions: (i) there are no discontinuities (in the sense of gross non-uniformities) in the properties of the screen, (ii) the probability of light absorption is small compared with the probability of scattering and (iii) solutions are sought for points far from the source [13, 14].

The MTF of the phosphor screen can be derived by summing (6) over the total screen thickness T and over the X-ray spectral distribution $f(E)$, and by normalising to zero spatial frequency, that is

$$\text{MTF}(u) = \frac{\sum_E \sum_T f(E)n_Q(E, T)q(t, E)m_0(E)G_1(\sigma, \beta, \varrho, u, t)}{\sum_E \sum_T f(E)n_Q(E, T)q(t, E)m_0(E)G_1(\sigma, \beta, \varrho, 0, t)}. \quad (9)$$

The NPS(u, E, t) of a phosphor screen may be defined as the spatial frequency distribution of the variance in the emitted optical photons over the screen area. The NPS associated with the emitted optical photons generated at depth t and escaping to the output may be written as follows [9, 13, 14]

$$\text{NPS}(u, E, t) = f(E)n_Q(E, T)q(t, E) \times [m_0(E)G_1(\sigma, \beta, \varrho, u, t)]^2. \quad (10)$$

The total screen NPS(u) can be obtained by summing over the screen thickness and the X-ray spectral distribution, as follows

$$\text{NPS}(u) = \sum_E \sum_T f(E)n_Q(E, T)q(t, E) \times [m_0(E)G_1(\sigma, \beta, \varrho, u, t)]^2. \quad (11)$$

Similar to MTF, a noise transfer function can be defined as [13, 14]:

$$\text{NTF}^2(u) = \frac{\sum_E \sum_T f(E)n_Q(E, T)q(t, E) [m_0(E)G_1(\sigma, \beta, \varrho, u, t)]^2}{\sum_E \sum_T f(E)n_Q(E, T)q(t, E) [m_0(E)G_1(\sigma, \beta, \varrho, 0, t)]^2}. \quad (12)$$

Finally Φ_1 can be calculated as:

$$\Phi_1 = \sum_E \sum_T f(E)n_Q(E, T)q(t, E)m_0(E)G_1(\sigma, \beta, \varrho, 0, t). \quad (13)$$

2.2 Experimental procedure

The scintillating screens were prepared in our laboratory by sedimentation of the phosphor powder (YAP: Ce-

Phosphor Technology Ltd, Code QM58/S-S1) on fused silica substrates (spectrosil B), with various coating weights ranging from 53 to 110 mg/cm², considered typical for use in various types of X-ray imaging applications. The density of this material was 4.15 g/ml, the mean particle size was 6.6 μm with a quartile deviation of 0.28 (Phosphor Technology Ltd., datasheet). Na₂SiO₃ was used as binding material between the powder particles.

The sedimentation technique employed for screen preparation, was as follows: A glass tube with 110 cm height and diameter of 5 cm was used. The tube was filled with a solution consisting of 1000 ml water, 20 ml of Na₂SiO₃, used as a binding material, and the phosphor powder mass. At the bottom of the tube a circular glass substrate of 3 cm diameter and of approximately 4.00 g of weight, was centrally placed. The solution was allowed to drip out slowly from the bottom of the tube. In this way a fraction of the initial phosphor mass was deposited on the glass substrate. The substrate and the phosphor were then weighted and the excess mass was accounted to the phosphor material. This mass was divided by the substrate surface and thus the surface density was determined.

The volume occupied by the phosphor grains on the glass substrate is considered to be approximately twice the volume that “pure” YAP:Ce would occupy, since the phosphor grains do not fit each other perfectly. Thus if a packing density of approximately 50% of YAP:Ce density is considered in the deposition process, then the phosphor layer thickness is obtained by dividing the calculated surface density with the corresponding packing density. In the case of the YAP:Ce phosphor, a surface density of 1 mg/cm² corresponding to approximately 5×10^{-4} cm of thickness.

The scintillating screens were irradiated by X-rays at various tube voltages (from 50 to 130 kV) employing a Philips Optimus X-ray radiographic unit. Tube filtration was 2.5 mm Al. Tube voltage was checked using an RMI model 240 multifunction meter. Incident exposure rate measurements were performed using a Radcal 2026C ionization chamber dosimeter (Radcal Corp. USA). An additional 20 mm Al filtration was introduced in the beam to simulate an average human body.

Absolute efficiency was determined by measuring the light energy flux emitted by the irradiated screen and dividing by the incident exposure rate, measured at screen position. The experimental set-up for light energy fluence measurements comprised a photomultiplier (EMI 9798 B) with an extended sensitivity S-20 photocathode and enclosed within a bronze light tight chamber [9, 11, 16–18]. The output current was amplified and fed to a vibrating reed (Cary 400) electrometer operated in current mode. An analogue to digital converter was employed to digitize electrometer’s output, which was then stored on a computer. Absolute efficiency was then computed from electrometer’s output current and dosimeter data by performing conversions and corrections according to the formula [15–17]

$$\text{AE} = \frac{i_{\text{elec}}(\text{pA})}{S n_p c_s c_g} \frac{1}{X}, \quad (14)$$

where i_{elec} is the electrometer’s output current in pA, S is the area of the irradiated screen and n_p is the photocathode’s

peak photosensitivity expressed in mA/W. c_s is the spectral compatibility factor expressing the compatibility of the scintillator's emission spectrum to the spectral sensitivity of the photocathode (extended S-20). c_s was determined by the relation [8, 16]

$$c_s = \frac{\int S(\lambda)D(\lambda) d\lambda}{\int S(\lambda) d\lambda}, \quad (15)$$

where $S(\lambda)$ is the scintillator's emission spectrum, measured by a method already described in previous work [14–17] and $D(\lambda)$ is the spectral sensitivity of the photodetector (photocathode), known from manufacturers datasheet. c_g is the geometric light collection efficiency of the experimental set-up, expressing the fraction of screen's emitted light incident on the photocathode. This fraction has been determined by taking into consideration: a) the angular distribution of the light emitted by the screen, which was obtained from literature [19] and b) the distance between the screen and the photocathode. Finally X , in (14), is the measured incident X-ray exposure rate.

For DQE evaluation, the factor $F\left(\frac{d\phi_1}{dF}\right)$ in (12), expressing the number of light photons emitted per incident X-ray, was calculated. The total light fluence emitted, Φ_1 was obtained via the absolute efficiency measurements. That is

$$\Phi_1 = \frac{AE \times X}{E_\lambda}, \quad (16)$$

where the nominator of (16) corresponds to the total light energy flux emitted through the screen surface and the de-

nominator is the mean energy of the optical photon emitted. The number of the incident X-ray photons was calculated via the X-ray spectrum [18]. The factors MTF and NPS were calculated by means of (9) and (11). The value of DQE for zero spatial frequency was calculated by means of (4) by taking into account that $MTF(0) = 1$ and $NTF(0) = 1$. Hence $DQE(0) = F\left(\frac{d\phi_1}{dF}\right)^2 \frac{MTF(0)^2}{NPS(0)NTF(0)^2}$, or $DQE(0) = F\left(\frac{d\phi_1}{dF}\right)^2 \frac{1}{NPS(0)}$. NPS(0) was theoretically determined by means of (11).

3 Results and discussion

In order to theoretically investigate the response of YAP:Ce, (2) was fitted to experimental data, obtained by (14), by trial and error. The fitting was performed by first selecting appropriate values for the parameters n_C , t_r , ρ and β in (2), while parameter σ was allowed to vary. First the value of n_C was chosen regarding the fact that the photon yield of the single-crystal YAP:Ce scintillator is 10 000 photons/Mev at 300 K [Marketech International, Inc. www.mkt-intl.com). Then by employing (6) and taking into account that the mean optical photon energy of YAP:Ce was calculated as 3.11 eV, a value of 0.031 was estimated for n_C . This value of n_C is close to values previously reported for other Ce activated phosphors (i.e., YAG:Ce), which range between 0.0139 to 0.05 [16, 18]. However, phosphors doped with different activators (i.e., $Gd_2O_2S:Tb$, $La_2O_2S:Tb$ and $ZnSCdS:Ag$) have been reported to exhibit n_C values as high as 0.20 [8, 10, 11]. The rest of the values (t_r , ρ and β) required for the fitting pro-

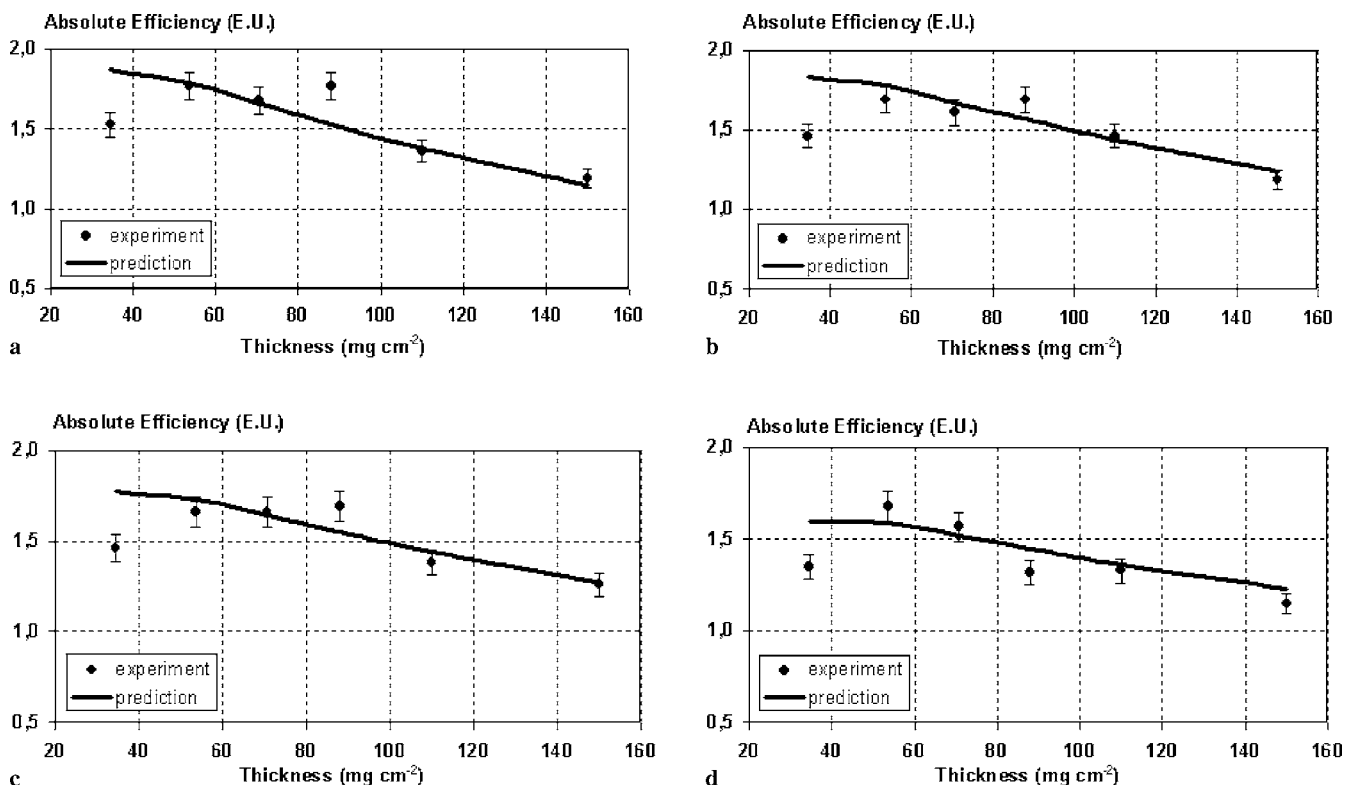


FIGURE 1 Comparison of absolute efficiency experimental and fitted results of the YAP:Ce phosphor screens irradiated with X-ray spectra of (a) 60 kVp, (b) 70 kVp, (c) 80 kVp and (d) 100 kVp respectively

cedure, were taken for previous studies [9–11, 14–16, 18] and were set as follows: $t_r = 0.3$, $\rho = 0.9$, $\beta = 0.03$. Using these data, we obtained the fitting of (2) to experimental values for values of σ varying between $91 \text{ cm}^2/\text{g}$ and $109 \text{ cm}^2/\text{g}$, with a mean value of $104 \text{ cm}^2/\text{g}$. This value corresponds to an optical linear attenuation coefficient equal to 219 cm^{-1} . This value of σ is higher than the corresponding value of other phosphors [9–11, 14–16, 18]. Since σ is a function of the optical photons scatter and absorption coefficients [9–11, 13, 14], a high σ value implies higher optical photon scatter and absorption within the phosphor material. The attenuation characteristics of the light in the phosphor screen are attributed mainly to the presence of the phosphor grains and less to the presence of the binding material. However the binding material affects the direction of the optical photon after a scattering event. The magnitude of the effect depends upon the ratio of the refractive index of the grain over the refractive index of the binding material [21]. In Fig. 1a to d the comparison between the AE experimental results and the calculated data, for $\sigma = 104 \text{ cm}^2/\text{g}$ is demonstrated.

Figure 2 shows the variation of experimental absolute luminescence efficiency of YAP:Ce powder scintillating screens with increasing X-ray tube peak voltage. The AE values were determined by means of (3), and they are expressed in efficiency units (EU, $1 \text{ EU} = 1 \mu\text{W m}^{-2}/\text{mR}$). It can be observed that increasing tube voltage lowers the absolute efficiency. This occurs because at higher X-ray energies fewer X-ray photons are absorbed in the phosphor, due to the decreasing mass energy absorption coefficient. A point worth noticing in Fig. 2 is that the absolute efficiency at 100 kVp is higher than the absolute efficiency at 90 kVp despite the fact that the X-ray energy absorbed at 100 kVp is lower. This occurs because at higher energies the depth of X-ray interaction increases and the optical photons are created closer to the phosphor’s emitting surface. Therefore the fraction of escaping optical photons is larger. On the other hand the number of optical photons produced at 90 kVp is larger, due to the higher X-ray absorption at lower energies. However the value $\sigma = 104 \text{ cm}^2/\text{g}$ found for the optical attenuation coefficient, suggests high scattering and absorption of these photons,

Photoreceptor	matching factor
GaAs	0.91
ES-20	0.98
Si	0.24
S9	0.87
KodakGR	0.99
GaAsP	0.40
S1133	0.51
a-Si104H	0.45
a-Si108H	0.45
S1227BR	0.47
S1337BR	0.32
S100AF	0.14
S100AB	0.86
a-Si	0.49
Agfa GS	0.99
Fuji	0.98

TABLE 1 Calculated matching factor of YAP:Ce with various photoreceptors

while they propagate to the exit; thus, fewer optical photons escape to the output at 90 kVp X-ray spectrum as compared to the 100 kVp X-ray spectrum. The absolute luminescence efficiency values, measured in this study for YAP:Ce phosphor, are comparable with the corresponding values reported for other Ce activated phosphors (i.e., YAG:Ce), which were studied under diagnostic radiology conditions [17].

In Table 1 the spectral compatibility of YAP:Ce, calculated with the use of (15), with various photodetectors is shown. It may be observed that YAP:Ce matches well with several radiographic films as well as with the ES-20 and S100AB photodetectors. Figure 3 demonstrates the calculated ratio MTF/NTF, which is utilized in (4), for the $53 \text{ mg}/\text{cm}^2$, $88 \text{ mg}/\text{cm}^2$ and $150 \text{ mg}/\text{cm}^2$ YAP:Ce phosphor screens irradiated with X-ray spectra of 60 kVp. As can be observed, the three curves are very close. Specifically the areas under the corresponding MTF curves, that were calculated by (9), present an overall difference of less than 0.36%. This may be explained by taking into account that the signal and noise transfer properties are principally affected by the directivity of light generation and the light attenuation effects (scatter-

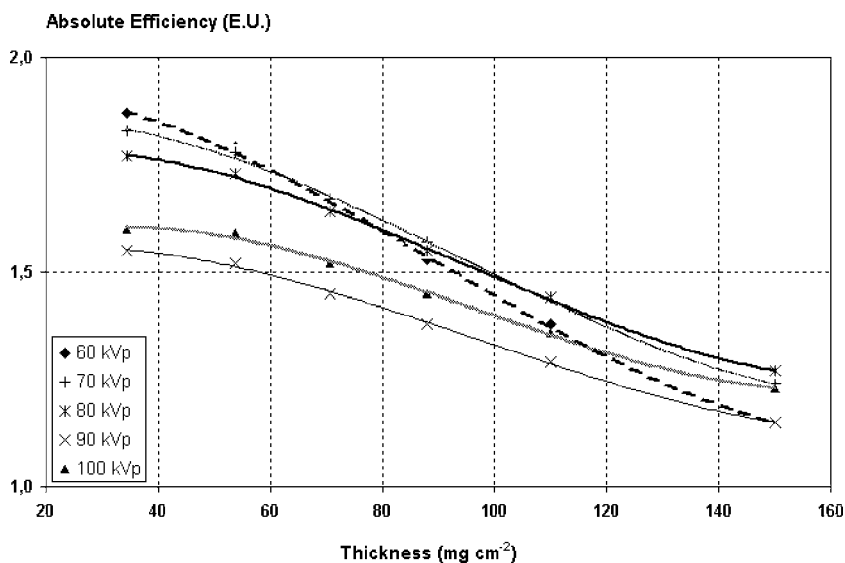


FIGURE 2 Theoretical calculation of YAP:Ce absolute efficiency of various surface densities, for X-ray spectra ranging between 60 kVp to 100 kVp

ing and absorption) within the phosphor material, especially for the fraction of the laterally directed optical photons that arrive at the screen emissive surface. These photons spread out on the screen surface and cause image quality degradation. The amount of these photons depends upon the phosphor thickness and the optical properties of the phosphor material, i.e., the energy E_λ of optical photons. For the YAG:Ce phosphor this energy lies in the region of “blue” light suggesting higher light scattering and larger light spread within phosphor’s mass. However, due to this spread, light photon trajectories are elongated leading to a higher absorption probability, especially for the laterally propagating optical photons. This effect, which is more pronounced in thicker screens, tends to limit light spread on the screen emitting surface. On the other hand, within thin screens, lateral light photons travel short distances to arrive at the screen surface. This also tends to limit output light spread. Therefore the output light burst may present a more or less similar shape in both thick and thin screens, for high σ values. This may also explain why the 88 mg/cm² curve is below the other two curves. That is

the shape of the light bursts emerging at the surface of the 53 mg/cm² phosphor screen are narrower due to the smaller distance the light travels to the phosphor exit. Additionally the light bursts of the 150 mg/cm² phosphor screen are also narrower in shape, as compared to the 88 mg/cm² phosphor. This is because laterally directed light photons suffer strong optical attenuation along their trajectories the screen emitting surface. It can also be observed from Fig. 3 that the MTF/NTF ratio is degraded with respect to spatial frequency. This may be explained by the fact that NTF, see (11) and (12), can be expressed as the weighted sum of the squares of the thin layers MTFs [22]. These MTFs are affected by the shape of the output light bursts, as it has already been noted. However the degradation of NTF with frequency is slower than the corresponding MTF degradation since the latter is expressed a weighted sum of the MTFs of each thin layer, thus the noise is transferred better than the signal with respect to spatial frequency [9–13, 22, 23].

In Fig. 4 the DQE values for zero spatial frequency, i.e., $DQE(0)$, of the YAP:Ce are presented. It is observed that the

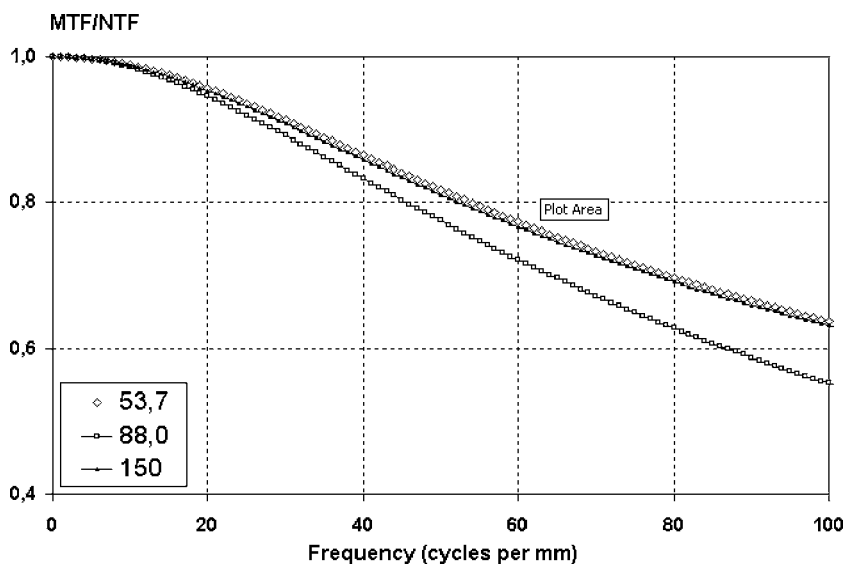


FIGURE 3 The calculated ratio of MTF over NTF (MTF/NTF) of three YAP:Ce phosphors, corresponding to coating thickness values of 53.7, 88.0 and 150 mg/cm², irradiated at 60 kVp

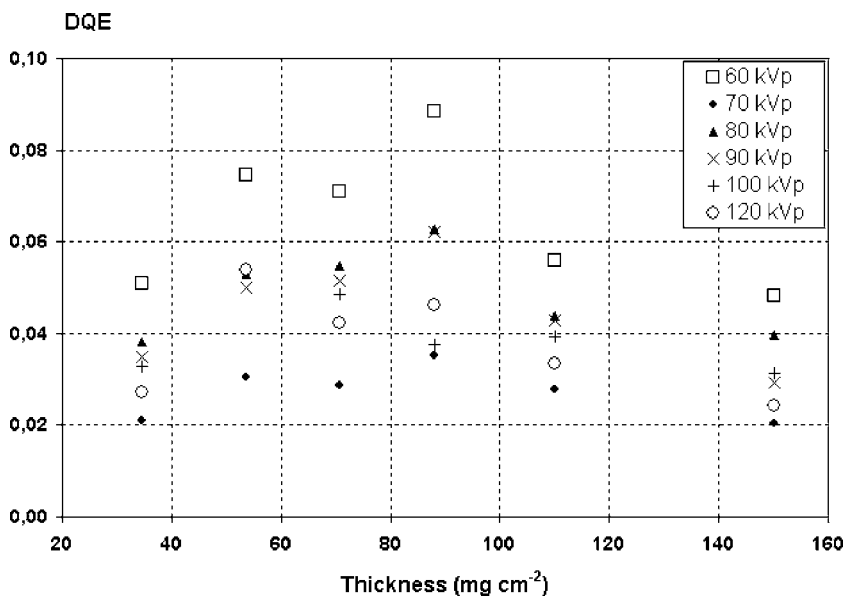


FIGURE 4 The zero spatial frequency DQE derived results of YAP:Ce phosphor screens of various surface densities, for X-ray spectra ranging between 60 kVp to 120 kVp

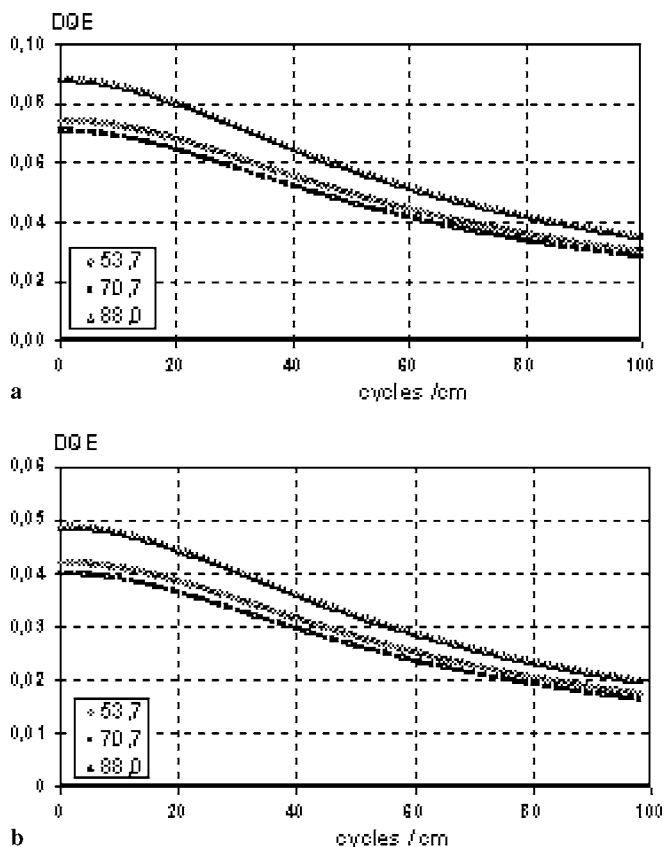


FIGURE 5 The frequency depended DQE derived results of YAP:Ce phosphor screens of various surface densities, irradiated with X-ray spectra of 60 kVp and 70 kVp, respectively

highest DQE values are observed for the X-ray energy of 60 kVp. This implies that the SNR transfer is more effective in this energy, due to the higher absorption of X-rays in the energy of 60 kVp with regard to higher energies. The DQE values calculated are lower than the corresponding values that have been reported for other materials, studied under medical X-ray conditions [11–16, 18]. This is mainly due to its moderate intrinsic efficiency ($n_c = 0.031$), as compared to phosphors doped with different activators (e.g., Tb, Tl, Ag), as well as to its high optical photon absorption characteristics, due to the low wavelength of the light created within this phosphor.

In Fig. 5a and b the spatial frequency dependent DQE for the X-ray energies of 60 kVp and 70 kVp is demonstrated. It may be observed that the higher DQE values are presented for the 88 mg/cm² phosphor screen. It may be observed that the DQE values are reduced with spatial frequency. This may be explained by the fact that DQE is proportional to the ratio of MTF over NTF and the degradation of NTF with frequency is slower than the corresponding MTF degradation [18, 20], thus the detectors ability to distinguish small details through image noise for high spatial frequencies is reduced.

4 Conclusion

In this study the cerium-doped yttrium aluminium oxide YAP:Ce powder scintillator was evaluated for use in X-ray imaging detectors. It was found that YAP:Ce matches well with various photodetectors. Absolute efficiency was

found to decrease with X-ray tube voltage for for YAP:Ce phosphor. Highest experimental efficiency was obtained for the 53.7 mg/cm² and 88.0 mg/cm² YAP:Ce screens. The optical parameters n_c and σ were found as 0.031 and 104.3 cm²/g, respectively. The high value of σ suggests higher optical photon absorption and scatter in the phosphor material. The signal and noise transfer characteristics of YAP:Ce were found to be affected more by the optical properties of the material than by its X-ray absorption properties. The highest DQE value was found for the 88 mg/cm² screen irradiated at 60 kVp. The imaging performance of YAP:Ce was comparable or lower to currently employed scintillators, however due to their fast response and high spectral compatibility to optical sensors they may be considered for use in digital imaging detectors.

ACKNOWLEDGEMENTS This work was financially supported by the Greek Ministry of Education (program EPEAEK ‘Archimidis’).

REFERENCES

- 1 J.A. Rowlands, J. Yorkston, In: *Handbook of Medical Imaging, Vol. 1, Physics and Psychophysics*, ed. by J. Beutel, H.L. Kundel, R.L. Van Metter (SPIE Press, Bellingham, 2000), pp. 234–248
- 2 C.W.E. van Eijk, *Phys. Med. Biol.* **47**, R85 (2002)
- 3 G. Blasse, B.C. Grabmaier, *Luminescent Materials* (Springer, Berlin Heidelberg, 1994)
- 4 A. Gorin, K. Kuroda, I. Manuilov, A. Riazantsev, T. Ishikawa, H. Kamitsubo, M. Suzuki, H. Toyokawa, *Nucl. Instrum. Methods A* **510**, 76 (2003)
- 5 K. Hirota, H. Toyokawa, M. Suzuki, T. Kudo, M. Nomachi, Y. Sugaya, M. Yosoi, A. Gorin, I. Manuilov, A. Riazantsev, K. Kuroda, *Nucl. Instrum. Methods A* **510**, 83 (2003)
- 6 M. Moszynski, M. Kapusta, D. Wolski, W. Klamra, B. Cederwall, *Nucl. Instrum. Methods A* **404**, 157 (1998)
- 7 M. Nikl, E. Mihokova, J.A. Mares, A. Vedda, M. Martini, K. Nejezchleb, K. Blazek, *Phys. Stat. Solidi* **181**, R10 (2000)
- 8 N. Kalivas, I. Valais, G. Salemis, C. Karagiannis, A. Konstantinidis, D. Nikolopoulos, G. Loudos, N. Sakelios, N. Karakatsanis, K. Nikita, V.L. Gayshan, A.V. Gektin, I. Sianoudis, N. Giokaris, C.D. Nomicos, N. Dimitropoulos, D. Cavouras, G. Panayiotakis, I. Kandarakis, *Nucl. Instrum. Methods A* **569**, 210 (2006)
- 9 I. Kandarakis, D. Cavouras, G.S. Panayiotakis, C.D. Nomicos, *Phys. Med. Biol.* **42**, 1351 (1997)
- 10 N. Kalivas, L. Costaridou, I. Kandarakis, D. Cavouras, C.D. Nomicos, G. Panayiotakis, *Nucl. Instrum. Methods A* **490**, 614 (2002)
- 11 I. Kandarakis, D. Cavouras, C.D. Nomicos, G.S. Panayiotakis, *Radiat. Meas.* **33**, 217 (2001)
- 12 J.H. Hubbell, S. M Seltzer, Tables of X-ray mass attenuation coefficients and mass energy absorption coefficients 1 keV to 20 MeV for elements $Z = 1$ to 92 and 48 additional substances of dosimetric interest, <http://physics.nist.gov/PhysRefData/XrayMassCoef/cover.html>
- 13 R.M. Nishikawa, M.J. Yaffe, *Med. Phys.* **16**, 773 (1989)
- 14 R.M. Nishikawa, M.J. Yaffe, *Med. Phys.* **17**, 894 (1990)
- 15 I. Kandarakis, D. Cavouras, D. Nikolopoulos, A. Anastasiou, E. Ventouras, I. Kalatzis, N. Dimitropoulos, N. Kalivas, G. Panayiotakis, *Radiat. Meas.* **39**, 263 (2005)
- 16 I. Kandarakis, D. Cavouras, C.D. Nomicos, G.S. Panayiotakis, *Nucl. Instrum. Methods B* **179**, 215 (2001)
- 17 I. Kandarakis, D. Cavouras, C.D. Nomicos, G.S. Panayiotakis, *Appl. Phys. B* **72**, 877 (2001)
- 18 <http://www.healthcare.siemens.com/med/rv/spektrum/radIN.asp>
- 19 I. Kandarakis, D. Cavouras, D. Nikolopoulos, A. Episkopakis, N. Kalivas, P. Liaparinos, I. Valais, G. Kagadis, K. Kourkoutas, I. Sianoudis, N. Dimitropoulos, C. Nomicos, G. Panayiotakis, *Appl. Radiat. Isotopes* **64**, 508 (2006)
- 20 I. Kandarakis, D. Cavouras, C.D. Nomicos, A. Bakas, G.S. Panayiotakis, *Nucl. Instrum. Methods A* **538**, 615 (2005)
- 21 P. Liaparinos, I. Kandarakis, D. Cavouras, H.B. Delis, G.S. Panayiotakis, *Med. Phys.* **34**, 1724 (2007)
- 22 G.J. Lubberts, *J. Opt. Soc. Am. A* **58**, 1475 (1968)
- 23 A. Badano, R.M. Gagne, B.D. Gallas, R.J. Jennings, J.S. Boswell, K.J. Myers, *Med. Phys.* **31**, 3122 (2004)